Published online September 14, 2017

RESEARCH

Genetic Characterization of Stem Rust Resistance in a Global Spring Wheat Germplasm Collection

Liangliang Gao, Matthew N. Rouse, Paul D. Mihalyov, Peter Bulli, Michael O. Pumphrey, James A. Anderson*

ABSTRACT

Stem rust, caused by the fungus *Puccinia graminis* Pers. f. sp. *tritici* Ericks, is one of the most damaging diseases of wheat (*Triticum aestivum* L.). The recent emergence of the stem rust Ug99 race group poses a serious threat to world wheat production. Utilization of genetic resistance in cultivar development is the optimal way to control stem rust. Here, we report association mapping of stem rust resistance in a global spring wheat germplasm collection (2152 accessions) genotyped with the wheat iSelect 9K single-nucleotide polymorphism array. Using a unified mixed model method (or QK method), we identified a total of 47 loci that were significantly associated with various stem rust resistance traits including field disease resistance and seedling resistance against multiple stem rust pathogen races including BCCBC, TRTTF, TTKSK (Ug99), and TTTTF. The 47 loci could be further condensed into 11 quantitative trait locus (QTL) regions according to linkage disequilibrium information among adjacent markers. We postulate that these QTLs represent known stem rust resistance genes including *Sr2*, *Sr6*, *Sr7a*, *Sr8a*, *Sr9h*, *Sr13*, *Sr28*, and *Sr36*. We further employed a multilocus mixed model to explore marker-trait associations and identified two additional QTLs (one potentially represents *Sr31*) that were significantly associated with stem rust resistance against various races. Combinations of the most significant loci for each trait explained up to 38.6% of the phenotypic variance. Markers identified through this study could be used to track the genes or QTLs. Accessions with high numbers of resistance-associated alleles may serve as important breeding materials for stem rust resistance.

L. Gao, Dep. of Agronomy and Plant Genetics, Univ. of Minnesota, St. Paul, MN 55108; L. Gao, current address, Dep. of Plant Pathology, Kansas State Univ., Manhattan, KS 66502; M.N. Rouse, USDA-ARS Cereal Disease Laboratory and Dep. of Plant Pathology, Univ. of Minnesota, St. Paul, MN 55108; P.D. Mihalyov, P. Bulli, and M.O. Pumphrey, Dep. of Crop and Soil Sciences, Washington State Univ., Pullman, WA 99164; J.A. Anderson, Dep. of Agronomy and Plant Genetics, St. Paul, MN 55108. Received 10 Mar. 2017. Accepted 13 July 2017. *Corresponding author (ander319@umn.edu). Assigned to Associate Editor Liuling Yan.

Abbreviations: AM, association mapping; BLAST, Basic Local Alignment Search Tool; BLUE, best linear unbiased estimate; COI, coefficient of infection; coi.BLUE, best linear unbiased estimate of stem rust field coefficient of infection trait; GWAS, genomewide association study; IT, infection type; it.BLUE, best linear unbiased estimate of stem rust field infection response trait; IWGSC, International Wheat Genome Sequencing Consortium; KASP, Kompetitive allele specific polymerase chain reaction; LD, linkage disequilibrium; LOESS, locally weighted polynomial regression; MAS, marker assisted selection; MLMM, multilocus mixed model; PCA, principal component analysis; *Pgt*, wheat stem rust fungus *Puccinia graminis*; QGLM, generalized linear model was investigated with a population structure adjustment; QK, a genomewide association study method accounting for both population structure and kinship ; QQ, quantile-quantile; QTL, quantitative trait locus; sev.BLUE, best linear unbiased estimate of stem rust field severity; SNP, single-nucleotide polymorphism.

Stem rust, caused by the fungus *Puccinia graminis* Pers. f. sp. *tritici* Ericks (*Pgt*), is one of the most damaging diseases of wheat (*Triticum aestivum* L.), dating back at least 3300 yr (Kislev, 1982; Chaves et al., 2013), and can cause disease epidemics in all wheat growing regions of the world (Roelfs, 1985; McIntosh and Brown, 1997). Rust pathogens have the ability to evolve within a short period of time to overcome plant resistance. A recent example is the emergence of the highly virulent *Pgt* race TTKSK (also

Published in Crop Sci. 57:2575–2589 (2017).
doi: 10.2135/cropsci2017.03.0159

known as Ug99) and related races in East Africa (Jin et al., 2008; Newcomb et al., 2016). The Ug99 race group can infect ~90% of the world's currently grown wheat acres and poses a serious threat to world wheat production (Singh et al., 2011; Singh et al., 2015). The most economical and environmentally sustainable way to control stem rust is through the development of resistant wheat varieties. So far, >60 genes conferring resistance to stem rust have been characterized and named (McIntosh et al., 1995; McIntosh et al., 2013; Yu et al., 2014). Many of these genes are race specific, meaning that the resistance they confer could become ineffective within a short period of time as a result of the frequent emergence of more virulent races of the pathogen. Gene pyramiding of multiple resistance genes might prove to be more durable (Mago et al., 2010).

In recent years, quantitative trait locus (QTL) mapping and tagging major genes with DNA markers have resulted in new tools for rust resistance breeding. Single-nucleotide polymorphisms (SNPs) have become a reliable choice for enriching genetic maps and developing markers for marker assisted selection (MAS) (Semagn et al., 2014). The use of high-density SNP markers to characterize resistance alleles in breeding populations provides breeders with a set of tools to conduct MAS and enhance the development of resistant varieties. One way to efficiently characterize resistance alleles in diverse germplasm is through association mapping (AM), also known as linkage disequilibrium (LD) mapping (Zhu et al., 2008). The rapid advancement of high-density marker platforms as well as AM model improvements have made genomewide association studies (GWAS) a powerful tool for characterizing marker-trait relationships. The resulting SNPs from GWAS analysis could potentially be used to develop markers with diagnostic haplotypes for target genes. Accessions with a high number of favorable alleles could be directly used as potential sources of disease resistance in breeding programs. Moreover, with recent advances in molecular breeding, the SNPs discovered with GWAS could potentially be incorporated into genomic selection models to accelerate crop trait prediction and selection (Rutkoski et al., 2011, 2012; Spindel et al., 2015, 2016).

Various successful GWAS analyses on wheat rust resistance have been conducted (Bajgain et al., 2015b; Maccaferri et al., 2015; Bulli et al., 2016; Gao et al., 2016; Turner et al., 2016b). Multiple GWAS studies have assessed stem rust resistance in the International Maize and Wheat Improvement Center germplasm (Crossa et al., 2007; Yu et al., 2011, 2012). Zhang et al. (2014) employed mostly simple sequence repeat markers to detect stem rust resistance alleles in a collection of US winter wheat and identified loci potentially representing stem rust resistance genes *Sr6*, *Sr24*, *Sr31*, *Sr36*, *Sr38*, and $Sr1RS^{Amigo}$. Bajgain et al. (2015b) employed the recently available wheat 90K SNP chip to identify resistance loci in a collection of North American spring wheat breeding lines and cultivars and detected genes *Sr2*, *Sr7a*, *Sr8a*, and *Sr11*, as well as other potentially novel loci. Similarly, GWAS of wheat stem rust resistance has been completed for Canadian wheat germplasm (Singh et al., 2013). However, to the best of our knowledge, no GWAS study has been conducted for stem rust resistance in a global spring wheat germplasm collection with entries from all major wheat growing regions. In addition, most of the AM studies for rust resistance primarily employed the QK method, a mixed model that accounts for both population structure (*Q*) and kinship (*K*) within populations (Zhang et al., 2014; Bajgain et al., 2015b; Maccaferri et al., 2015). All associations in QK analysis are based on single marker tests. Segura et al. (2012) suggest that the multilocus mixed model (MLMM) could outperform the QK method, especially for traits controlled by several large effect loci. Compared with single marker analysis, MLMM analysis could lead to higher power and lower false discovery rates by factoring (causative) genomewide loci into stepwise regression analysis (Segura et al., 2012).

The current study includes an approximately 10-fold greater number of breeding lines than previous stem rust AM studies (Yu et al., 2011, 2012; Zhang et al., 2014; Bajgain et al., 2015b). This larger population studied could potentially boost our power to detect rare resistance alleles. The goals of this study were to characterize the stem rust resistance alleles present in a global spring wheat collection, and to identify novel stem rust resistance loci that could potentially be used in molecular breeding efforts. We also explored the use of the more recent MLMM model for detecting marker-trait associations. This study is expected to broaden our understanding of stem rust resistance and assist breeders in developing wheat cultivars with effective and durable stem rust resistance.

MATERIALS AND METHODS

Plant Materials

As part of the Triticeae Coordinated Agricultural Project, 3042 spring wheat accessions were assembled by the USDA-ARS Small Grains and Germplasm Research Unit. Of these accessions, 2188 were genotyped using the wheat iSelect 9K SNP array (Cavanagh et al., 2013). After quality filtering on the basis of 9K genotyping results (see genotyping section for details), a total of 2152 accessions were retained for subsequent analysis. The 2152 accessions represented a worldwide collection of spring wheat from 108 countries located in four continents: Europe (22.1%), Asia (33.5%), Africa (20.1%), and the Americas (21.8%). The GWAS panel was composed of 489 breeding lines, 422 cultivars, 383 cultivated materials, 9 genetic stocks, and 849 landraces (Supplemental Table S1).

Stem Rust Phenotyping

The 3042 accessions were grown under greenhouse conditions and inoculated after full emergence of the primary leaf 7 to 10 d

after, planting according to Rouse et al. (2011), in five independent tests of *Pgt* races BCCBC (isolate 09CA115-2), TRTTF (06YEM34-1), TTKSK (Ug99, 04KEN156/04), TTTTF (01MN84A-1-2), and a race mixture using six US *Pgt* races also used in field inoculations: MCCFC (59KS19), QFCSC (06ND76C), QTHJC (75ND717C), RCRSC (77ND82A), RKQQC (99KS76A), and TPMKC (74MN1409). Readers are referred to a list of publications discussing the virulence and avirulence formulae of these isolates, including recently emerged *Pgt* races and their variants (Rouse et al., 2011; Olivera et al., 2012; Singh et al., 2015; Bhattacharya 2017).

Seedling infection types (IT) were scored 12 to 14 d after inoculation according to the 0-to-4 scale developed by Stakman et al. (1962). The phenotype data were converted to a linearized 0-to-9 scale using a custom Perl script (Gao et al., 2016).

For the field studies, the accessions were planted in single rows in the field and inoculated with the *Pgt* race mixture (see above) ~1 mo after planting when the entries started to tiller (Feekes Growth Stage 2–3) (Large 1954). Phenotyping was conducted ~1 mo after inoculation. Disease severity and infection response were recorded according to Rouse et al. (2011) in four different years (2011–2014) at one location (St Paul, MN). For the first and fourth year, only about half of the 2152 accessions (982 for Year 1 and 1170 for Year 4) were evaluated, since the Triticeae Coordinated Agriculture Project panel was expanded in 2012. The phenotypic data were converted to three measures (severity, infection response, and coefficient of infection [COI]) using a separate custom Perl script designed for field data conversion (Gao et al., 2016). The field phenotypic values were further adjusted based on a mixed linear model, with environments as random effects, and genotypes as having fixed effects. Best linear unbiased estimates (BLUEs), calculated using the "lme4" package of the open source statistical language or software environment R (R Core Team 2015) were used to represent genotype performance across different environments. Estimated stem rust disease phenotypes for 2152 accessions are listed in Supplemental Table S1.

DNA Extraction, Genotyping Platform, and Reference Linkage Maps

Genomic DNA was extracted from seedling plants using the cetyl trimethylammonium bromide (CTAB) method as described in Maccaferri et al. (2015) and genotyped with the Illumina's iSelect 9K SNP array at the USDA-ARS Biosciences Research Laboratory in Fargo, ND. Out of the 2188 accessions, 2152 were retained for GWAS after removing accessions with >10% missing data. A total of 6223 SNP markers were retained for GWAS after filtering based on minor allele frequency ($\geq$0.05) and missing data percentage ($\leq$10%). For map positions of the filtered SNPs, we used the published consensus map for the wheat 9K SNP array (Cavanagh et al., 2013) with reversed orientations of chromosomes 4A, 5A, and 5B, as reported in Maccaferri et al. (2015). Additionally, based on comparative alignment to the published wheat 90K SNP map (Wang et al., 2014) and Basic Local Alignment Search Tool (BLAST+ command line version 2.2.28) hit information on International Wheat Genome Sequencing Consortium (IWGSC) reference genome contigs (Consortium 2014), we joined fragmented linkage groups with a spacing of 20 cM for linkage groups 3D (3D1, 3D2, and 3D3), 5D (5D1cult [reversed], 5D2cult, and 5D3cult) and 6D (6D1 and 6D2 [reversed]). A final version of the modified 9K consensus map used in this study, as well as comparisons with the wheat 90K map and IWGSC contigs based on BLAST hits, are listed in Supplemental Table S2.

We also genotyped our GWAS panel using known markers linked to *Sr2*, *Sr36*, and *Sr28*. Two Kompetitive allele specific polymerase chain reaction (KASP) assays wMAS000005 (*Sr2*) (Mago et al., 2011) and wMAS000015 (*Sr36*) (MAS Wheat, 2016), along with an agarose gel based marker WSUSr28 for *Sr28* (forward: ACCCCATTTGGCAGGTGAAA, reverse: TTCGACGAATCCACAAGGCA, with resistant allele product of 500 bp and susceptible allele product of 400 bp; Bajgain et al., 2015b), were used in the genotyping. The approximate positions of *Sr36* and *Sr28* were estimated at 70 and 240 cM on chromosome 2B based on published studies (Tsilo et al., 2008; Babiker et al., 2017). To illustrate, IWB55504, a 90K SNP marker (not included in 9K consensus map) associated with *Sr28* (Babiker et al., 2017), is located at 134.5 cM on the 90K map (Wang et al., 2014). We can estimate the equivalent 9K position to be around 240 cM based on the collinear 9K and 90K relationships established in Supplemental Table S2. The differences of 9K and 90K positions are due to scaling differences. This study adopted the modified 9K consensus map positions (Supplemental Table S2; Cavanagh et al., 2013) instead of the 90K map positions, since the published 90K map (Wang et al., 2014) did not incorporate all of the 9K loci into consensus order. The recently developed KASP assay for *Sr28* (Babiker et al., 2017) was not available at the time when our experiments were performed. Gene *Sr2* is located at ~15 cM on 3B in the 9K map. The markers wMAS000005, wMAS000015, and WSUSr28 were used as positive controls in our GWAS analysis and were not subject to minor allele frequency filtering steps.

Population Structure, Kinship, and Linkage Disequilibrium Analysis

To obtain highly informative and nonredundant SNPs for population structure analysis, the SNP marker data were pruned using PLINK software v1.9 (Purcell et al., 2007). The command line option for pruning was "–indep-pairwise 100 5 0.2." A total of 1532 markers were retained after pruning. The pruned set of SNPs were used for population structure (*Q*) analysis using a model-based clustering method in STRUCTURE v2.3.4 (Pritchard et al., 2000) and a principal component analysis (PCA) method in R. The PCA plots were color coded according to STRUCTURE results of membership assignments. For the model-based structure analysis, a total of 10 independent runs were conducted for each specified *K* (number of subpopulations), with 25,000 burn-in length and 50,000 Markov chain Monte Carlo iterations. The most likely number of clusters (*K*) was chosen based on the ΔK method (Evanno et al., 2005), implemented in a web-based informatics tool "Structure Harvester" (Earl and vonHoldt, 2012). CLUMPP (Jakobsson and Rosenberg, 2007) software v1.1 was used to consolidate STRUCTURE runs to derive the **Q** matrix used in AM. A kinship matrix (**K**) for line relatedness was calculated in TASSEL (Bradbury et al., 2007) according to the scaled (or centered) identity-by-state method using the whole set of SNP markers that passed quality filtering. Pairwise marker LD was

also calculated using TASSEL v4.3.13. The LD decay curves were fitted for each subgenome (A, B, or D) separately using a locally weighted polynomial regression (LOESS) function in R. Similar to previous studies (Pasam et al., 2012, Gao et al., 2016), here we used a LD r^2 value of 0.2 as a critical level for defining LD decay.

Marker-Trait Association Analysis Based on Mixed Linear Mmodels, Generalized Linear Mmodels with Population Structure as a Covariate, and a Multilocus Mixed Model Approach

To examine the genetic basis of stem rust resistance in this panel, a QK-based unified mixed linear model was first applied with population structure estimates (*Q*) included as fixed effects and kinship (*K*) as random effects (Yu et al., 2006). Additionally, the use of a generalized linear model was investigated with a population structure adjustment (QGLM) method using TASSEL v4.3.13 (Bradbury et al., 2007). The model components for QK analysis were previously described (Bernardo, 2010; Gao et al., 2016). The MLMM (Segura et al., 2012) was then applied using a set of R functions (MLMM software, 2012) open sourced by Segura et al. (2012). This method applies a stepwise MLMM regression in structured populations (kinship and population structure can be accounted simultaneously). The maximum number of steps of MLMM analysis was set at 10. Optimal results of MLMM were determined based on Bonferroni corrections.

Marker-trait association test *p*-values, R^2, and marker effects were extracted from TASSEL runs or MLMM analysis. For multiple test correction of QK results, we first explored the use of *simpleM* method (SimpleM software, 2008) (Gao et al., 2008, 2010, 2016; Hirsch et al., 2014) to denote significance of marker-trait associations. Stepwise regressions (Cantor et al., 2010; Gao et al., 2016) were performed on loci detected based on the *simpleM* threshold. However, to be consistent in multiple test correction methods between different models (QK vs. MLMM), we later adopted the Bonferroni method ($0.05/6226 = 8.03 \times 10^{-6}$) to denote significance of marker-trait associations. The R^2 values from LD analysis were used in conjunction with genetic distances to assign cosegregating or adjacent significant markers into a unique QTL block.

QTL-Tagging SNPs, Multiple Regressions, and Gene Postulations

The most significant marker for each LD block or QTL region was selected to represent each QTL. Resistance-associated allele frequencies in the GWAS population or subpopulations were counted for the most significant markers of each QTL region. The multiple regression method was further employed to calculate combined effects (or the percentage of variation explained) of multiple markers (QTLs). Loci postulations were conducted primarily based on marker positions (including BLAST hit contig arm assignments) and existing knowledge of IT patterns for different *Pgt* races.

RESULTS

Population Structure Analysis

The 2152 accessions used for GWAS analysis in this study were composed of breeding lines, cultivars, cultivated lines, genetic stocks, and landraces from 108 countries (Fig. 1). The model-based structure analysis revealed that the panel can be divided into two subpopulations based on the Evanno ΔK method. Whereas most of European and American accessions were grouped into Subpopulation 1, Subpopulation 2 consisted of accessions predominantly from Iran and India, with few accessions from other Asian and African countries. (Fig. 1 and 2). The presence of two subpopulation groups in the panel was also confirmed by PCA, suggesting that the use of a QK model with either PCA or *Q* as a covariate is expected to produce consistent results, as previously revealed in a similar study (Gao et al., 2016). In this study we used the **Q2** matrix from the model-based population structure analysis for correcting population structure in GWAS analysis.

Seedling and Field Stem Rust Disease Phenotypes

The responses of seedling plants to single *Pgt* races were generally skewed toward susceptible types (Fig. 3). A higher frequency of resistant or immune accessions (>300) were observed for response to race BCCBC (Fig. 3). The field response of adult plants to the *Pgt* race mixture (as measured by percentage severity and COI) showed near-normal distributions (Fig. 3). The phenotypic correlations among various field and seedling phenotypes are significant, with race TTKSK as the exception (Table 1). Seedling responses to race TTKSK had lower correlations with responses to other races (Table 1). Among the three field traits (BLUEs for infection response [it.BLUE], stem rust field severity [sev.BLUE], and COI [coi.BLUE]), the field infection response type (it.BLUE) has the highest correlations to seedling ITs ($R = 0.59$ for race.mix-it.BLUE [linearized seedling rust scores in response to race mixture inoculations and adult plant response type in the field] and $R = 0.6$ for BCCBC-it.BLUE [linearized seedling rust scores in response to race BCCBC and adult plant response type in the field] (Table 1).

Correlation and heritability analysis for field stem rust disease phenotypes revealed that the year-to-year correlations for adult plant stem rust traits were highly significant ($p < 2.2 \times 10^{-16}$) and the heritability values for these traits were fairly high. The Pearson's correlations are 0.61, 0.68, and 0.71, and the heritability values are 0.82, 0.84, and 0.89 for the three traits (severity, COI, and IT), respectively. These values are comparable with those for stripe rust (caused by *Puccinia striiformis* Westend.) GWAS studies on global spring or winter wheat germplasm collections (Maccaferri et al., 2015; Bulli et al., 2016).

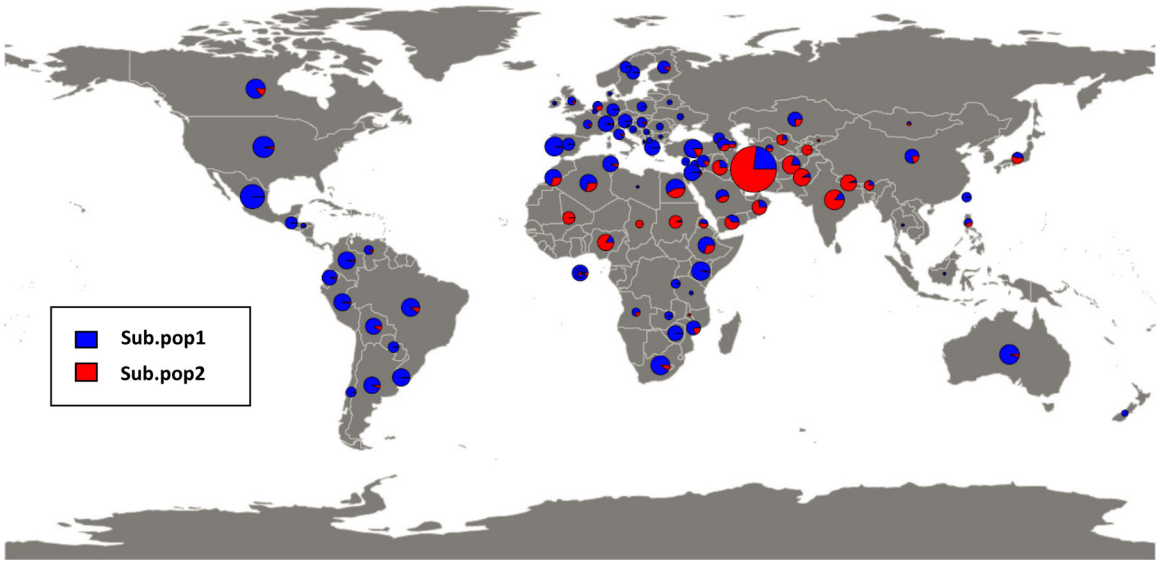

Fig. 1. Country-specific distributions of population structure subgroups of the worldwide panel of 2152 spring wheat accessions. Pie charts show the percentage subpopulation (sub.pop) compositions for given countries.

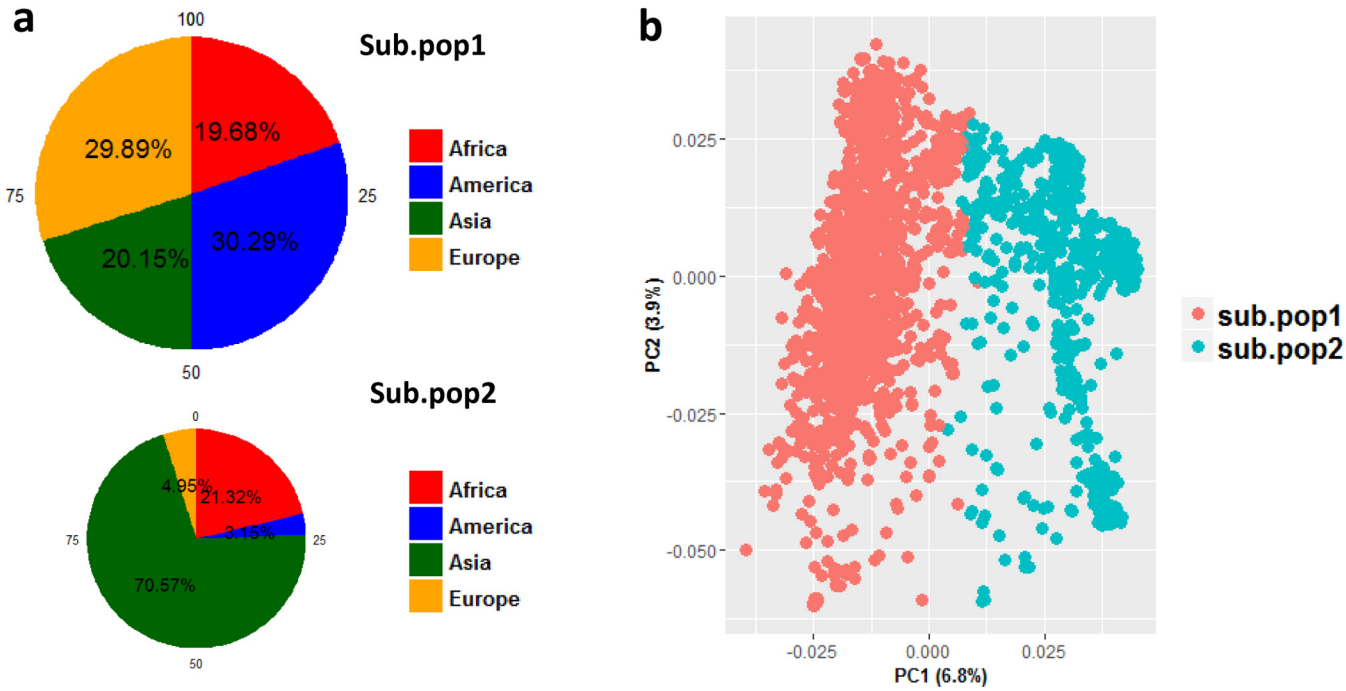

Fig. 2. (a) Four major continental origins of accessions used in this study, visualized in red (Africa), blue (America), green (Asia), and yellow(Europe) colors for each subpopulation (sub.pop). Most of European and American accessions belong to Subpopulation1, whereas more than half of Subpopulation 2 consists of accessions collected from Asia with some from Africa. (b) Two subpopulations derived from Structure v2.3.4 analysis, visualized (red and blue) on principal component (PC) analysis plot.

Analysis of variance and multiple test comparison analysis of sev.BLUE revealed that the breeding lines and genetic stocks displayed the highest rust resistance levels (26.4 on a 0–100 scale), followed by cultivars (35.4), landraces (38.6), and cultivated materials (41.4). Within each subpopulation, however, the differences between cultivars and landraces were not statistically significant based on Tukey's honest significant difference test. Consistent results were also observed for it.BLUE and coi.BLUE traits.

Genomewide Marker Coverage and Linkage Disequilibrium

After quality filtering, a total of 6226 markers were retained for GWAS analysis. These markers spanned a genetic distance of 3603 cM based on the modified 9K consensus map (Supplemental Table S2). The average number of markers per centimorgan was 1.99 and 2.12 for the A and B genomes, respectively. In contrast, the average number of markers for the D genome was 0.42 cM^{-1} (or one marker every 2.4 cM). Though the D genome

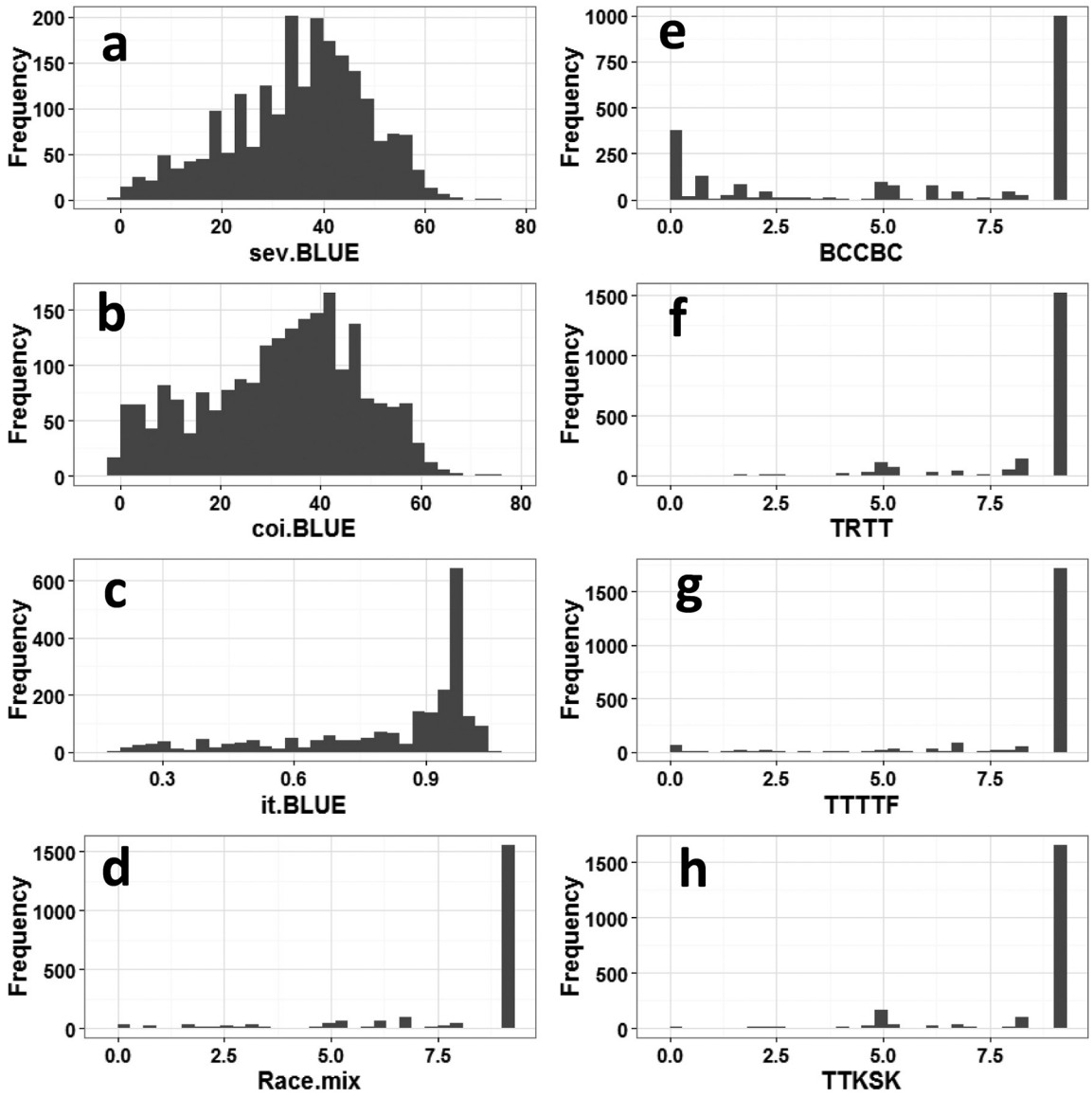

Fig. 3. Disease distributions for field and seedling traits. (a–c) Field disease distributions measured by percentage severity, coefficient of infection, and linearized (0–1) infection response type (see Gao et al. 2016 for details on conversions). (d) Seedling disease distributions for the race mixture. (e–h) Seedling response distributions for single races: BCCBC, TRTTF, TTTTF, and TTKSK. The phenotype distributions in response to single races are skewed toward susceptibility (with BCCBC as a possible exception, with additional frequencies for immune types). sev.BLUE, best linear unbiased estimate of stem rust field severity; coi.BLUE, best linear unbiased estimate of stem rust field coefficient of infection trait; it.BLUE, best linear unbiased estimate of stem rust field infection response trait.

Table 1. Correlations among field and seedling stem rust phenotypes. Diagonal lower left side shows Pearson's correlation *R* values. Diagonal upper right side denotes the *p*-values for each correlation.

Traits†	sev.BLUE	coi.BLUE	it.BLUE	Race.mix	BCCBC	TRTTF	TTTTF	TTKSK
sev.BLUE	1	$<2.2 \times 10^{-16}$	$<2.2 \times 10^{-16}$	$<2.2 \times 10^{-16}$	$<2.2 \times 10^{-16}$	$<2.2 \times 10^{-16}$	$<2.2 \times 10^{-16}$	6.11×10^{-6}
coi.BLUE	0.98	1	$<2.2 \times 10^{-16}$	$<2.2 \times 10^{-16}$	$<2.2 \times 10^{-16}$	$<2.2 \times 10^{-16}$	$<2.2 \times 10^{-16}$	4.35×10^{-5}
it.BLUE	0.77	0.85	1	$<2.2 \times 10^{-16}$	$<2.2 \times 10^{-16}$	$<2.2 \times 10^{-16}$	$<2.2 \times 10^{-16}$	3.10×10^{-4}
Race.mix	0.46	0.50	0.59	1	$<2.2 \times 10^{-16}$	$<2.2 \times 10^{-16}$	$<2.2 \times 10^{-16}$	2.44×10^{-2}
BCCBC	0.55	0.59	0.60	0.43	1	$<2.2 \times 10^{-16}$	$<2.2 \times 10^{-16}$	1.43×10^{-9}
TRTTF	0.34	0.36	0.40	0.39	0.41	1	$<2.2 \times 10^{-16}$	1.88×10^{-2}
TTTTF	0.37	0.40	0.46	0.37	0.39	0.39	1	3.55×10^{-2}
TTKSK	0.10	0.09	0.08	0.05	0.13	0.05	0.05	1

† sev.BLUE, best linear unbiased estimate of stem rust field severity; coi.BLUE, best linear unbiased estimate of stem rust field coefficient of infection trait; it.BLUE, best linear unbiased estimate of stem rust field infection response trait; Race.mix, linearized seedling rust scores in response to race mixture inoculations.-

had the lowest density coverage, this was expected and consistent with previous reports (Cavanagh et al., 2013; Wang et al., 2014; Maccaferri et al., 2015; Gao et al., 2016). Linkage disequilibrium decayed at 7.4 and 4.3 cM for the A and B genomes, respectively, and at 10 cM for the D genome (Fig. 4). The high LD in the D genome practically reduces the number of markers required for association tests. We also observed a moderate to high LD among SNP markers mapped to the paracentromeric or even distal regions of chromosome 2B. For example, Markers IWA2739 and IWA1114, located at 146.6 and 94.01 cM on 2B, respectively, were in high LD (r^2 = 0.4), and the two markers wMAS000015 (*Sr36*) and WSUSr28 (*Sr28*) were in LD ($r^2 > 0.1$) despite being located on different chromosome arms.

Marker-Trait Associations Based on QK, QGLM, and MLMM Analysis

Inclusion of both *Q* and *K* into the GWAS analysis in this study significantly reduced the chance for false marker-trait associations. For QK results, the expected −log10(*p*) values and observed −log10(*p*) values are close to the diagonal reference (*X* = *Y*) line on the quantile-quantile (QQ) plot for larger *p*-values (lower left on QQ plot) (Supplemental Fig. S1). The distribution of *p*-values from QGLM analysis skewed upwards in the QQ plot (results not shown), suggesting the presence of more false positives (Type I error). The QK model is generally favored when compared with the QGLM model; therefore, we adopted the *p*-values from QK to determine significance of loci in single marker tests.

For QK analysis, a total of 47 markers were significantly associated with stem rust resistance (*p*-values passing the Bonferroni corrected threshold) (Supplemental Fig. S2). The *p*-values for the 47 marker associations with various traits are listed in Supplemental Table S3. The 47 loci can be further condensed into 11 regions based on LD values of adjacent markers. The 11 regions with significant marker-trait association *p*-values for various traits are listed in Table 2.

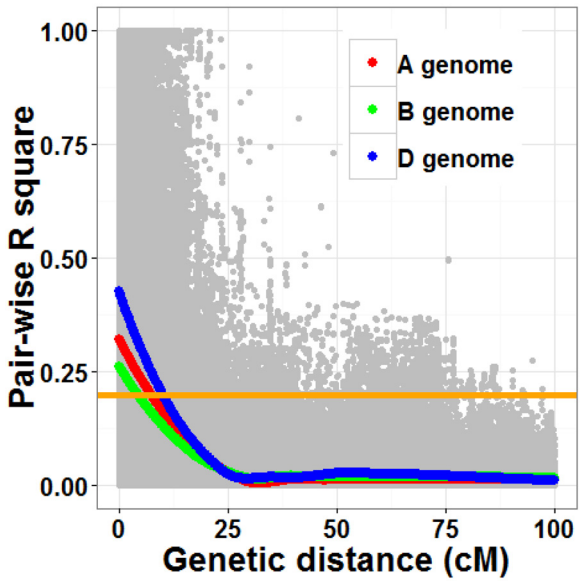

Fig. 4. Genome wide linkage disequilibrium (LD) decays based on 9K genotyping results. The LD decayed rapidly for the A and B genomes, but slower for D genomes. The orange bar indicates LD decay level, r^2 = 0.2.

For MLMM analysis, a total of 13 QTLs were significantly associated with stem rust resistance to various *Pgt* races and under seedling or adult plant developmental stages (Fig. 5, Table 3). The MLMM results and QK results often agreed with each other. For example, all of the 11 QK loci were detected in MLMM analysis (Table 3). For specific traits, the exact loci compositions for QK and MLMM models might be different. For example, for the sev.BLUE trait, the QK model detected two genes, *Sr2* and *Sr36*, whereas the MLMM model also detected these two genes but with an additional QTL 2B.3. For the TTTTF trait, the QK model detected 4A.1 and 4A.2 (*Sr7a*), whereas the MLMM model detected an additional QTL 1B.1A (likely *Sr31*). For TTKSK trait, the QK model detected *Sr36*, *Sr28*, *Sr9h*, and *Sr13*, whereas the MLMM model detected *Sr28*, *Sr9h*, and potentially novel loci (2B.2, 2B.3).

Gene Postulations for Field and Seedling Resistance Loci

Overall, significant loci were detected for seven traits (sev.BLUE, coi.BLUE, it.BLUE, BCCBC, TRTTF, TTKSK, and TTTTF) based on QK analysis. The percentage variation explained by each locus (R^2 values) varied between 0.5 and 14.8% (Table 2). Gene names for these loci were postulated (Table 2) based on the 9K consensus map position information (chromosome arms and previously published map locations) and race specificity.

Based on previously published map locations and race specificity, the QTLs identified in this study—4A.1, 6A.1, 2B.4, 2B.5, 2D.1, and 6A.2—likely correspond to the seedling resistance genes *Sr7a* (Bajgain et al., 2015b; Turner et al., 2016a), *Sr8a* (Bajgain et al., 2015b; Dunckel et al., 2015; Guerrero-Chavez et al., 2015), *Sr9h* (Rouse et al., 2014; Babiker et al., 2016), *Sr28* (Rouse et al., 2012; Babiker et al., 2017), *Sr6* (Tsilo et al., 2010), and *Sr13* (Simons et al., 2011), respectively. The QTLs 4A.1, and 6A.1 explained 6.0 and 7.5% of the observed phenotypic variance in response to the races TTTTF and TRTTF, respectively. QTLs 2B.4 and 2B.5 accounted for 3.8 and 14.8% of the genetic variance, respectively, in response to TTKSK (Ug99); and 2B.2 and 2D.1 accounted for 3.4 and 2.5% of the observed variations, respectively, in response to BCCBC.

For field resistance, two loci (likely *Sr2* and *Sr36*) were consistently detected for different traits (sev.BLUE, coi.BLUE, and it.BLUE) (Table 2). The presumed *Sr2* and *Sr36* loci explained 7.6 and 3% of the variation for the sev.BLUE trait, respectively (Table 2). The percentage of the variation explained was fairly similar for coi.BLUE (7.1 and 2.2%).

Table 2. Most significant quantitative trait loci (QTL) for each trait based on QK model (a genomewide association study method accounting for both population structure and kinship), ordered by trait and loci position. The *p*-values are based on QK method.

Trait†	QTL	Markers	Chromosome	Position	*p*	R^2	Effect	Resistance allele	Favorable allele frequency			Gene	References
									Whole population	Subpopulation 1	Subpopulation 2		
sev.BLUE	2B.1	wMAS000015	2B	70.00	2.69×10^{-7}	0.030	19.56	T	0.014	0.016	0.009	*Sr36*	Tsilo et al., 2008
sev.BLUE	3B.1	wMAS000005	3B	15.00	1.89×10^{-35}	0.076	15.06	T	0.052	0.074	0.004	*Sr2*	Mago et al., 2011
coi.BLUE	2B.1	wMAS000015	2B	70.00	1.47×10^{-5}	0.022	18.36	T	0.014	0.016	0.009	*Sr36*	Tsilo et al., 2008
coi.BLUE	3B.1	wMAS000005	3B	15.00	1.23×10^{-33}	0.071	16.24	T	0.052	0.074	0.004	*Sr2*	Mago et al., 2011
it.BLUE	2B.1	wMAS000015	2B	70.00	1.50×10^{-4}	0.015	0.22	T	0.014	0.016	0.009	*Sr36*	Tsilo et al., 2008
it.BLUE	2B.2‡	IWA8599	2B	70.19	7.18×10^{-4}	0.005	0.04	C	0.232	0.305	0.072	‡	–
it.BLUE	3B.1	wMAS000005	3B	15.00	1.07×10^{-56}	0.126	0.29	T	0.052	0.074	0.004	*Sr2*	Mago et al., 2011
BCCBC	2B.2‡	IWA8599	2B	70.19	3.94×10^{-17}	0.034	1.61	C	0.232	0.305	0.072	‡	–
BCCBC	2B.5	WSUSr28	2B	240.00	1.25×10^{-6}	0.024	2.28	§	0.040	0.055	0.009	*Sr28*	Baigain et al., 2015b
BCCBC	2D.1	IWA6897	2D	77.18	1.85×10^{-12}	0.025	1.69	A	0.131	0.156	0.075	*Sr6*¶	Tsilo et al., 2010
BCCBC	3B.1	wMAS000005	3B	15.00	2.00×10^{-4}	0.007	1.02	T	0.052	0.074	0.004	*Sr2*	Mago et al., 2011
BCCBC	6A.1	IWA7913	6A	9.54	2.97×10^{-7}	0.012	0.96	G	0.174	0.210	0.096	*Sr8a*	Guerrero-Chavez et al., 2015
TRTTF	6A.1	IWA5781	6A	2.21	7.30×10^{-35}	0.075	2.06	T	0.093	0.133	0.004	*Sr8a*	Guerrero-Chavez et al., ,2015
TRTTF	6A.2	IWA7495	6A	216.09	3.88×10^{-8}	0.015	0.90	G	0.058	0.068	0.036	*Sr13*	Simons et al., 2011
TTTTF	4A.1	IWA6696	4A	183.69	1.61×10^{-28}	0.060	1.62	T	0.128	0.179	0.016	*Sr7a*	Turner et al., 2016a
TTTTF	4A.2	IWA5353	4A	205.62	2.36×10^{-9}	0.017	0.57	A	0.309	0.339	0.244	*Sr7a*	Turner et al., 2016a
TTKSK	2B.1	wMAS000015	2B	70.00	1.13×10^{-19}	0.102	5.40	T	0.014	0.016	0.009	*Sr36*	Tsilo et al., 2008
TTKSK	2B.3‡	IWA4532	2B	94.01	2.57×10^{-6}	0.010	0.85	C	0.112	0.150	0.027	‡	–
TTKSK	2B.4	IWA4294	2B	192.19	5.67×10^{-19}	0.038	0.91	C	0.540	0.464	0.713	*Sr9h*	Babiker et al., 2017
TTKSK	2B.5	WSUSr28	2B	240.00	4.68×10^{-27}	0.148	3.17	‡	0.040	0.055	0.009	*Sr28*	Baigain 2015b
TTKSK	6A.2	IWA7495	6A	216.09	8.21×10^{-5}	0.007	0.70	G	0.058	0.068	0.036	*Sr13*	Simons et al., 2011

† sev.BLUE, best linear unbiased estimate of stem rust field severity; coi.BLUE, best linear unbiased estimate of stem rust field coefficient of infection trait; it.BLUE, best linear unbiased estimate of stem rust field infection response trait.

‡ Potentially novel stem rust resistance loci.

§ WSUSr28 is an agarose gel marker instead of a single-nucleotide polymorphism (SNP) marker, with a resistant allele product of approximately 500 bp, and a susceptible allele product of ~400 bp.

¶ The location of the SNPs corresponds to the location of *Sr6* on 2DS (see Supplemental Table S3 for details), but not *Sr54* on 2DL (Ghazvini et al. 2013).

The variation explained by *Sr2* was 12.6% for infection response (it.BLUE) (Table 2). The resistant (or favorable) allele frequencies for *Sr2* and *Sr36* were 5.2 and 1.4% respectively (Table 2).

The results from MLMM analysis revealed QTLs that were mostly in similar locations to QTLs derived from the QK analysis. The MLMM loci detected likely represent genes *Sr2*, *Sr6*, *Sr7a*, *Sr8a*, *Sr9h*, *Sr13*, *Sr28*, and *Sr36* (Table 3). The *p*-values from MLMM analysis were highly significant (ranged from 6.4×10^{-6} to 2.3×10^{-61}) (Table 3). Significant associations involving the loci *IWA2057* and *IWA5702* on chromosome 1AS were also identified. However, *IWA2057* and *IWA5702* were correlated with other loci on chromosome 1BS. Molecular analysis using the microsatellite marker SCM9 (Weng et al., 2007), diagnostic for the 1BL.1RS translocation, suggests that these markers represent *Sr31* (Mihalyov et al., 2017).

Cumulative Effects of Most Significant Loci

Under multiple regression models, the most significant markers altogether (Table 2) explained 12.1, 11.5, 18.5, 16.4, 24.6, 19.2, and 27.4% of the phenotypic variation for the seven traits (sev.BLUE, it.BLUE, coi.BLUE, BCCBC, TRTTF, TTTTF, and TTKSK, respectively), after correcting for population structure.

The number of resistance-associated marker alleles and disease resistance levels were correlated for each trait, with accessions having higher numbers of resistance-associated alleles observed as generally more resistant. For example, the correlation between the number of resistance-associated alleles and sev.BLUE, coi.BLUE, and it.BLUE phenotypic values are $r = 0.41$, 0.40, and 0.36, respectively. The *p*-values for these correlation tests are all highly significant ($p < 0.001$). Accessions with multiple resistance-associated alleles could serve as important breeding material. For example, we identified lines with both of the resistance-associated alleles for TRTTF resistance

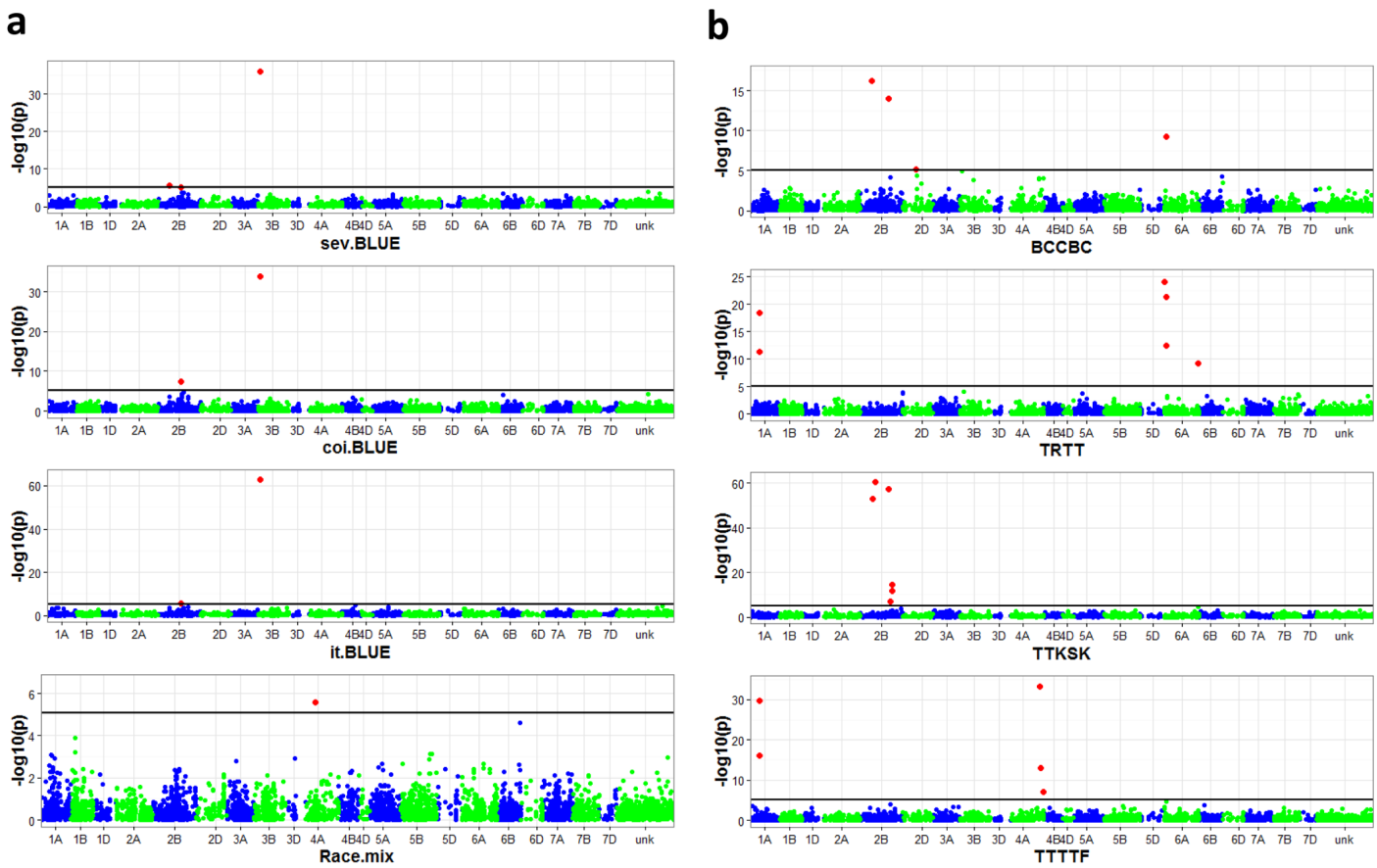

Fig. 5. Manhattan plots based on the multilocus mixed model for (a) race mix traits (including best linear unbiased estimated field severity [sev.BLUE], coefficient of infection [coi.BLUE], and response type [it.BLUE]) and (b) single races BCCBC, TRTTF, TTKSK, and TTTTF.

(Supplemental Table S4). We also identified 49 and 34 lines that have three or more of the resistance-associated alleles for BCCBC and TTKSK resistance (Supplemental Table S4). Considering the 13 QTLs together (regardless of traits), we were able to identify >100 accessions with six to eight resistance-associated alleles (Supplemental Table S5). These accessions could be used as valuable sources of resistance to stem rust, including the TTKSK race, in breeding and/or genetic studies.

For MLMM analysis, loci were identified for each of the traits sev.BLUE, it.BLUE, coi.BLUE, Race.mix(linearized seedling rust scores in response to race mixture inoculations), BCCBC, TRTTF, TTTTF, and TTKSK. These loci explained 18.5, 25.9, 17.4, 4.5, 13.8, 34.8, 29.5, and 38.6% of phenotypic variation for each trait, respectively. The cumulative R^2 values were generally higher than the cumulative effects of the loci detected by QK analysis (see above).

DISCUSSION

Population Structure and Its Impact on Stem Rust Resistance

Here, we classified two primary subpopulations among the global spring wheat diversity panel: Asia and the West. These results coincide with several other studies that document the population genetics of worldwide wheat collections (Maccaferri et al., 2015; Bulli et al., 2016; Mihalyov et al., 2017). The STRUCTURE results possibly reflect the domestication and distribution history of modern wheat. Domestication started in West Asia, followed by spread to Europe, Africa, and the Americas. Extensive selections, mutations, and enrichment of favorable alleles followed the spread. New adapted varieties and breeding lines formed distinct population groups that differed from the Asian group.

The two subpopulations were associated with different stem rust resistance levels ($p < 0.001$). The phenotypic variances explained by population structure ranged from 0.8 to 26.2% for various traits, with TTKSK being the lowest and BCCBC being the highest. The average stem rust ratings for Subpopulation 1 (Europe and America) were lower than those for Subpopulation 2 (Asia), by 10.8 on a 0-to-100 scale for sev.BLUE, and by 1.36 on a 0-to-9 scale for seedling plants against Race.mix. It can be speculated that the higher resistance of Subpopulation 1 might be related with the fact that the races used in the race mixture in this study are North American races, and breeding lines in Subpopulation 2 (Asia and Africa) have not been selected for resistance to these races. Interestingly, for resistance to race TTKSK (Ug99), the Subpopulation 2

Table 3. Quantitative trait loci (QTL) detected under multi-locus mixed model (MLMM).

Trait†	QTL	Marker	Chromosome	Position	*p*-value	Gene	Reference
sev.BLUE	2B.1	wMAS000015	2B	70.00	2.25×10^{-6}	*Sr36*	Tsilo et al., 2008
sev.BLUE	2B.3‡	IWA2739	2B	146.60	6.04×10^{-6}	‡	–
sev.BLUE	3B.1	wMAS000005	3B	15.00	1.17×10^{-36}	*Sr2*	Mago et al., 2011
it.BLUE	2B.3‡	IWA3210	2B	147.63	2.19×10^{-6}	‡	–
it.BLUE	3B.1	wMAS000005	3B	15.00	9.54×10^{-64}	*Sr2*	Mago et al., 2011
coi.BLUE	2B.3‡	IWA2739	2B	146.60	4.67×10^{-8}	‡	–
coi.BLUE	3B.1	wMAS000005	3B	15.00	1.58×10^{-34}	*Sr2*	Mago et al., 2011
BCCBC	2B.2‡	IWA8599	2B	70.19	6.40×10^{-17}	‡	–
BCCBC	2B.5	WSUSr28	2B	240.00	9.47×10^{-15}	*Sr28*	Bajgain et al., 2015b
BCCBC	2D.1‡	IWA2415	2D	83.84	6.39×10^{-6}	*Sr6*	Tsilo et al., 2010
BCCBC	6A.1	IWA7913	6A	9.54	5.97×10^{-10}	*Sr8a*	Guerrero-Chavez et al., 2015
TTTTF	1B.1A	IWA2057	1A	57.95	6.57×10^{-17}	*Sr31*	Weng et al., 2007
TTTTF	1B.1A	IWA5702	1A	57.95	2.33×10^{-30}	*Sr31*	Weng et al., 2007
TTTTF	4A.1	IWA6696	4A	183.69	6.23×10^{-34}	*Sr7a*	Turner et al., 2016a
TTTTF	4A.1	IWA4651	4A	193.19	1.10×10^{-13}	*Sr7a*	Turner et al., 2016a
TTTTF	4A.2	IWA4083	4A	207.06	8.49×10^{-8}	*Sr7a*	Turner et al., 2016a
TTKSK	2B.2‡	IWA4531	2B	80.41	7.62×10^{-54}	‡	–
TTKSK	2B.3‡	IWA1114	2B	94.01	2.33×10^{-61}	‡	–
TTKSK	2B.4	IWA4294	2B	192.19	1.67×10^{-7}	*Sr9h*	Babiker et al., 2017
TTKSK	2B.4	IWA2676	2B	200.11	2.78×10^{-8}	*Sr9h*	Babiker et al., 2017
TTKSK	2B.4	IWA2677	2B	200.11	3.41×10^{-15}	*Sr9h*	Babiker et al., 2017
TTKSK	2B.5	WSUSr28	2B	240.00	5.54×10^{-58}	*Sr28*	Bajgain et al., 2015b
TRTTF	1B.1A	IWA2057	1A	57.95	5.26×10^{-12}	*Sr31*	Mihalyov et al., 2017
TRTTF	1B.1A	IWA5702	1A	57.95	3.71×10^{-19}	*Sr31*	Mihalyov et al., 2017
TRTTF	6A.1	IWA5781	6A	2.21	7.84×10^{-25}	*Sr8a*	Guerrero-Chavez et al., 2015
TRTTF	6A.1	IWA7006	6A	8.69	3.58×10^{-13}	*Sr8a*	Guerrero-Chavez et al., 2015
TRTTF	6A.1	IWA7913	6A	9.54	3.97×10^{-22}	*Sr8a*	Guerrero-Chavez et al., 2015
TRTTF	6A.2	IWA7495	6A	216.09	6.06×10^{-10}	*Sr13*	Simons et al., 2011
Race.mix	4A.m1‡	IWA8495	4A	63.29	2.70×10^{-6}	‡	–

† sev.BLUE, best linear unbiased estimate of stem rust field severity; coi.BLUE, best linear unbiased estimate of stem rust field coefficient of infection trait; it.BLUE, best linear unbiased estimate of stem rust field infection response trait; Race.mix, linearized seedling rust scores in response to race mixture inoculations.

‡ Potentially novel stem rust resistance loci.

(Asia) group showed an increased level of resistance (by 0.34 on a 0-to-9 scale, $p = 5.09 \times 10^{-5}$).

Stem Rust Phenotypes and Correlations

The high frequency of susceptible seedling plants (Fig. 3) to races TRTTF, TTTTF, and TTKSK was expected, as these selected races have previously been shown to be broadly virulent, and the majority of the accessions in this panel likely do not possess major resistance loci effective against these races. The relative high number of immune types (>300) for resistance to BCCBC was also expected, as BCCBC is the least virulent race examined in this study. The fact that field response phenotypes showed near-normal distributions could possibly suggest that, unlike seedling response to single races, field resistance is more quantitative in nature and likely controlled by many loci with small effects. The observation that infection response type shows the highest correlations to seedling ITs (0.59, 0.60) (Table 1) likely reflects the biology that both field infection response (it.BLUE) and seedling ITs were measured by rust pustule size, shape, and the degree of chlorosis in the surrounding area.

Extent of Linkage Disequilibrium and QTL Block Delineation

This study fitted LD decay curves using the LOESS function in R. The LOESS function returns fitted r^2 values and ranged from 0 to 0.32 for the A genome, 0 to 0.26 for the B genome, and 0 to 0.43 for the D genome. The selection of r^2 of 0.2 as the critical decay level was employed in various studies (Pasam et al., 2012; Gao et al., 2016) and deemed appropriate in the current study.

Interestingly, a cluster of QTLs or genes on chromosome 2B (2B.1 on *Sr36*; 2B.2, 2B.3, and 2B.4 on *Sr9h*; and 2B.5 on *Sr28*) were detected that confer resistance to various traits including sev.BLUE, coi.BLUE, BCCBC, and TTKSK (Table 2 and 3). Huang et al. (2012) discovered that the introgression of *Sr36* generates segregation distortion throughout the chromosome. This could be the cause of long range LD observed for QTL 2B.3 (94.01–146.6 cM) (Table 2 and 3). Quantitative trait loci on wheat chromosomes other than 2B generally comprised compact or sharply delineated LD blocks.

Genomewide Marker Trait Association Analysis

In this study, the wheat 9K SNP array and 2152 spring wheat accessions were used for GWAS analysis of stem rust resistance. First, we employed single marker tests using the QGLM and QK models, then we applied multiple regressions to examine cumulative effects of loci. We identified a total of 47 markers that were significantly (passing Bonferroni multiple-test correction threshold) associated with stem rust resistance to various races at the seedling stage and to a mixture of races in the field at the adult stage. The 47 markers can be collapsed into 11 QTL regions (Table 2) located on five chromosomes including 2B, 2D, 3B, 4A, and 6A. Interestingly, we were not able to detect loci effective for seedling response to a combination of six mixed races. This could be due to the *p*-value threshold being too stringent, or the race specificities of the races included in the mixture did not overlap.

Researchers have argued that correcting for marker effects based on both population structure and kinship could be overly conservative and might result in a need for relaxed *p*-values such as 0.001 or alternative ways to correct for background variations (Pasam et al., 2012; Bernardo, 2013; Zegeye et al., 2014). As an exploratory analysis, we lowered our significance threshold to the level determined by the *simpleM* method (Gao et al., 2008, 2010, 2016; Hirsch et al., 2014). This resulted in the detection of 24 QTLs in 12 chromosomes, with potentially novel loci on eight chromosomes. The QTLs were for all eight traits including the mixed-race seedling resistance, which was previously undetected using the more stringent Bonferroni threshold. The majority of the QTL regions associated with the field race mixture traits (sev.BLUE, coi.BLUE, it.BLUE, and Race.mix) are overlapping, whereas resistance loci associated with individual races are mostly nonoverlapping (Supplemental Fig. S3).

Using the Bonferroni correction threshold, the MLMM method generally agreed with the QK method for all the traits. All 11 QTLs identified through QK analysis were also identified in MLMM analysis. In general, the MLMM method identified a higher number of significant loci, including two new QTL regions (1B.1A and 4A.m1) (Table 2 and 3) that were not detected by the QK method. The cumulative effects of these significant loci for each trait were higher than those detected by the QK method. Gene *Sr2* appeared to be the most significant locus for field resistance both in QK and MLMM analyses. The differences in exact QTL compositions between QK and MLMM models could reflect the key differences between single marker analysis and stepwise regression as implemented in MLMM, where genomewide loci could serve as conditionals to remove false positives.

Comparison of *Pgt* Resistance QTLs with Known *Sr* Genes

In the current study, three genes—*Sr2*, *Sr28*, and *Sr36*—were tagged by markers wMAS000005, WSUSr28, and wMAS000015. Worldwide, gene *Sr2* has provided adult plant resistance to *Pgt* races for >60 yr (Ellis et al., 2014). Our study reveals that *Sr2* was present in ~5% of the worldwide diversity panel accessions. Importantly, our study also reveals that the majority of the *Sr2* accessions (108 of them) possess at least one other resistance-associated allele detected in this study (Supplemental Table S5). The joint use of *Sr2* together with other R genes or QTLs could potentially provide high levels of field rust resistance that would be useful for agriculture. Babiker et al. (2017) used the wheat 90K SNP platform to identify markers linked to *Sr28*. The majority of the markers identified were specific to the 90K platform, thus not directly comparable with the loci identified through this study. Nonetheless, based on approximate collinear relationships between 9K and 90K markers (Supplemental Table S2), we were able to project the position of *Sr28* (as well as WSUSr28) to be ~240 cM on the 9K consensus map. Most of the *Sr28* positive accessions postulated by Babiker et al. (2017) were not included in this panel except CITR7611, PI268468, PI572693, of which two (CITR7611 and PI572693) were also positive for *Sr28* based on WSUSr28 (QTL 2B.5, Supplemental Table S5). Gene *Sr36* confers resistance to predominant US wheat stem rust fungus races (Tsilo et al., 2008). The current study reveals that *Sr36* is present at low frequency (1.4%) (Table 2) in the worldwide diversity accessions.

Zurn et al. (2014) positioned the TTKSK resistance gene *SrWLR* with several SNP markers including IWA6121. The 9K position for those markers is 205 to 206 cM (Supplemental Table S2), which corresponded to the QTL region of 2B.4 of this study (likely *Sr9h*, Supplemental Table S3, Table 2 and Table 3). Babiker et al. (2016) used the 90K SNP platform to identify a locus derived from CItr4311, and the map position of that locus and infection patterns suggest that it is *Sr9h*. One of the markers, IWA7850, identified by Babiker et al. (2016), is shared with the current study, with resistance allele T and susceptible allele C, consistent with Babiker et al. (2016). Guerrero-Chavez et al. (2015) identified a TTKSK resistance locus from hard spring wheat line SD4279, which also corresponded to the QTL 2B.4 region of this study (Supplemental Table S3). Frequent detection of the *Sr9* locus through various studies likely suggests its role as an important source for TTKSK resistance. Furthermore, Naruoka et al. (2016) mapped a stripe rust resistance gene, *Yr5*, using the wheat iSelect 9K assay to approximately the same region as the *Sr9* locus, although the genetic relationships between *Yr5* and the *Sr9* locus remain to be elucidated.

In addition to the TTKSK resistance locus, Guerrero-Chavez et al. (2015) also identified a 6AS locus effective

against race TRTTF, with linked SNPs including the marker IWA7913, which was also identified in this study (Supplemental Table S3, Table 2 and 3). Consistent with previous reports, we postulate that this locus represents *Sr8a*. Postulations of the 6AS TRTTF resistance locus (as *Sr8a*) can also be found in an independent GWAS study of stem rust resistance in North American spring wheat breeding lines (Bajgain et al., 2015b). Approximately 17% (>300 lines) of the worldwide diversity accessions possess the resistance associated allele for *Sr8a*.

Turner et al. (2016a) used the wheat 9K chip to identify markers linked to *Sr7a* in the winter wheat cultivar Jagger. Two of the markers identified (IWA4084, IWA4858) were also detected in the current study for TTTTF resistance (Supplemental Table S3). The detection of *Sr7a* in not only biparental mapping populations, but also a large AM panel, suggests its effectiveness against TTTTF within a wide collection of germplasm. This study detected two adjacent loci for the *Sr7a* region (4A.1 and 4A.2). The detection of two loci instead of one locus could be related with the relatively high LD threshold (e.g., when compared with Zegeye et al., 2014) used to define QTL regions, or it could potentially indicate two adjacent loci that were jointly responsible for TTTTF resistance.

This study also identified loci that potentially represent genes *Sr6* (2D.1) and *Sr13* (6A.2). These postulations are based on projected position information based on published studies (Tsilo et al., 2010; Simons et al., 2011) and IT patterns. The *Sr6* and *Sr13* alleles were present in ~13 and 6% of the accessions studied (Table 2). The 2D.1 (*Sr6*) allele frequency in Subpopulation 1 is comparable with what was discovered in a previous AM study (Zhang et al., 2014). Two EST markers, CD926040 and BE471213, flanking *Sr13* (Simons et al., 2011) were mapped to chromosome 6A, between 613 and 616 Mb (IWGSC reference genome v1). Marker IWA7495 (6A.2, *Sr13*) was mapped to 615 Mb of chromosome 6A. These position results support our gene postulations. The current study could serve as a starting point to integrate various *Sr* genes into wheat consensus maps.

Some of the loci detected in this study, even when deemed independent by multiple or stepwise regression analysis, were mapped to the same or adjacent QTL intervals. For example, multiple 2B.4 loci (*Sr9h*) were detected through MLMM analysis (Table 3) and were tentatively annotated as *Sr9h*. It is very common for resistance genes to have multiple alleles. For example, the barley (*Hordeum vulgare* L.) *Mla* gene encodes >30 different specificities (Seeholzer et al., 2010). The wheat *Sr50* gene holds extensive haplotype diversity (Mago et al., 2015). The wheat *Sr9* locus encodes at least eight different alleles. Thus, even though loci deemed independent by multiple regression models were mapped to approximately the same position, they could be in LD with different *Sr* gene haplotypes.

In addition to known *Sr* genes, our study also revealed potentially novel loci on wheat chromosomes 2B and 4A (and more if using *simpleM* threshold). The QTL 2B.2 was located on the short arm of chromosome 2B (close to *Sr36*, but in different LD blocks) and was detected for it.BLUE and BCCBC traits (Tables 2 and 3). This locus is likely novel based on infection pattern and location information. The QTL 2B.3 was located in the proximal region of 2BS, (Supplemental Table S2, Table 2) and has a moderate effect (0.85 out of 1–9) on TTKSK resistance. This locus is >30 cM proximal (supplemental Table S1) from a recently detected 2B QTL effective against TTKSK (Bajgain et al., 2015a) and potentially represents a new gene. The QTL 4A.m1 was detected only when using the MLMM method (Table 3). This locus was significantly ($p < 0.001$) associated with resistance against race mixtures and likely represents a novel locus based on location information and IT pattern. As stem rust resistance in the field tended to be controlled by many loci with small effects, one way to employ these novel loci (and known *Sr* genes) is through inclusion of these QTL-tagging loci in genomic selection models to enable more accurate trait predictions (Rutkoski et al., 2011, 2012' Spindel et al., 2013, 2016; Thavamanikumar et al., 2015).

This study employed the (most) strict Bonferroni correction ($p = 8.03 \times 10^{-6}$) method to control for family wise error rate and a modest number of loci were detected. Indeed, using a relaxed threshold (e.g., the simpleM method) (Gao et al., 2008, 2016) reveals more loci (Supplemental Fig. S3). However, we preferred to use the stricter Bonferroni threshold to ensure that detected loci represent true loci. With the large germplasm collection and numerous potential historic recombination events present in this panel, the marker density provided by the 9K assay is likely still not large enough to capture all resistance loci. Higher-density genotyping assays such as the wheat 90K SNP chip, as well as genotyping by sequencing (Elshire et al., 2011) technologies could potentially fill this gap. The relatively few number of novel loci detected could be attributed to the limitation inherent in any AM study, namely the lack of capacity to detect rare alleles present in the population (Bernardo 2016).

This study was successful in detecting a number of known genes or QTLs (*Sr2*, *Sr7a*, *Sr8a*, *Sr9h*, *Sr28*, and *Sr36* etc.). The total number of potentially known loci detected (nine) is greater than most previous stem rust GWAS studies (Yu et al., 201; Zhang et al., 2014; Bajgain et al., 2015b). Characterization of known loci within a large collection of germplasm could potentially provide breeders a rich selection of lines with desired combinations of *Sr* genes to use in stem rust resistance breeding.

CONCLUSIONS

Our GWAS analysis detected multiple stem rust resistance genes, such as *Sr2*, *Sr6*, *Sr7a*, *Sr8a*, *Sr9h*, *Sr13, Sr28*, *Sr31*, and *Sr36* in 2152 accessions of a global spring wheat panel. Potentially novel resistance loci on chromosomes 2B and 4A were also identified. Most of the identified loci were effective against one or few, but not all, races or effective under one developmental stage (seedling vs. field). The cumulative effects of significant loci explained 4.5 to 25.9% of the phenotypic variation for resistance against race mixtures, whereas the proportion of variation explained for resistance against single races ranged from 13.8 to 38.6%. Loci identified in this study could potentially be converted to uniplex KASP assays to assist high-throughput marker assisted breeding. The accessions with a high number of favorable alleles can be used as important sources of stem rust resistance in breeding programs.

Conflict of Interest

The authors declare that there is no conflict of interest.

Supplemental Material Available

Supplemental material for this article is available online.

Author Contribution Statement

L. Gao performed data analysis steps including phenotype adjustment, population structure analysis, and marker trait associations. M.N. Rouse performed greenhouse and field stem rust experiments. L. Gap performed *Sr28* and *Sr36* genotyping on the population. P.D. Mihalyov and P. Bulli performed *Sr2* genotyping and population SNP calling (wheat 9K array). L. Gao drafted the first manuscript, M.N. Rouse, P.D. Mihalyov, P. Bulli, M.O. Pumphrey, and J.A. Anderson all contributed to the revision and writing of this manuscript. M.N. Rouse, M.O. Pumphrey, and J.A. Anderson conceived the project and provided guidance throughout project development.

Acknowledgments

This study is part of the Triticeae Coordinated Agriculture Project (www.triticeaecap.org), funded by USDA National Institute of Food and Agriculture Grant no. 2011-68002-30029. We thank Dr. Shiaoman Chao (USDA-ARS, Fargo, ND) for performing 9K SNP chip genotyping of the GWAS panel. We thank Sheri Rynearson (Washington State University) and Qi Wang (University of Minnesota) for technical assistance in DNA extractions and genotyping. We thank Dr. Katherine Frels (University of Minnesota) for reviewing an earlier draft of this manuscript. We acknowledge Amy Fox for facilitating the stem rust field and seedling experiments. Computing resources from the Minnesota Supercomputing Institute at the University of Minnesota are greatly appreciated.

References

Babiker, E.M., T. Gordon, S. Chao, M.N. Rouse, M. Acevedo, G. Brown-Guedira et al. 2017. Molecular mapping of stem rust resistance loci effective against the Ug99 race group of the stem rust pathogen and validation of a SNP marker linked to stem rust resistance gene *Sr28*. Phytopathology 107:208–215. doi:10.1094/PHYTO-08-16-0294-R

Babiker, E.M., T.C. Gordon, S. Chao, M.N. Rouse, R. Wanyera, M. Newcomb et al. 2016. Genetic mapping of resistance to the Ug99 race group of *Puccinia graminis* f. sp. *tritici* in a spring wheat landrace CItr 4311. Theor. Appl. Genet. 129:2161–2170. doi:10.1007/s00122-016-2764-5

Bajgain, P., M. Rouse, S. Bhavani, and J. Anderson. 2015a. QTL mapping of adult plant resistance to Ug99 stem rust in the spring wheat population RB07/MN06113-8. Mol. Breed. 35:170. doi:10.1007/s11032-015-0362-x

Bajgain, P., M. Rouse, P. Bulli, S. Bhavani, T. Gordon, R. Wanyera et al. 2015b. Association mapping of North American spring wheat breeding germplasm reveals loci conferring resistance to Ug99 and other African stem rust races. BMC Plant Biol. 15:249. doi:10.1186/s12870-015-0628-9 [erratum: 16:24].

Bernardo, R. 2010. Breeding for quantitative traits in plants. 2nd ed. Stemma Press, Woodbury, MN.

Bernardo, R. 2013. Genomewide markers for controlling background variation in association mapping. Plant Genome 6(1):1–9. doi:10.3835/plantgenome2012.11.0028

Bernardo, R. 2016. Bandwagons I, too, have known. Theor. Appl. Genet. 129:2323–2332. doi:10.1007/s00122-016-2772-5

Bhattacharya, S. 2017. Wheat rust back in Europe. Nature 542:145–146. doi:10.1038/nature.2017.21424

Bradbury, P.J., Z. Zhang, D.E. Kroon, T.M. Casstevens, Y. Ramdoss, and E.S. Buckler. 2007. TASSEL: Software for association mapping of complex traits in diverse samples. Bioinformatics 23:2633–2635. doi:10.1093/bioinformatics/btm308

Bulli, P., J. Zhang, S. Chao, X. Chen and M. Pumphrey. 2016. Genetic architecture of resistance to stripe rust in a global winter wheat germplasm collection. G3: Genes, Genomes, Genet. 6:2237–2253. doi:10.1534/g3.116.028407

Cantor, R.M., K. Lange, and J.S. Sinsheimer. 2010. Prioritizing GWAS results: A review of statistical methods and recommendations for their application. Am. J. Hum. Genet. 86:6–22. doi:10.1016/j.ajhg.2009.11.017

Cavanagh, C.R., S.M. Chao, S.C. Wang, B.E. Huang, S. Stephen, S. Kiani et al. 2013. Genome-wide comparative diversity uncovers multiple targets of selection for improvement in hexaploid wheat landraces and cultivars. Proc. Natl. Acad. Sci. USA 110:8057–8062. doi:10.1073/pnas.1217133110

Chaves, M.S., J.A. Martinelli, C. Wesp-Guterres, F.A.S. Graichen, S.P. Brammer, S.M. Scagliusi et al. 2013. The importance for food security of maintaining rust resistance in wheat. Food Secur. 5:157–176. doi:10.1007/s12571-013-0248-x

Consortium, T.I.W.G.S. 2014. A chromosome-based draft sequence of the hexaploid bread wheat (*Triticum aestivum*) genome. Science 345:1251788. doi:10.1126/science.1251788

Crossa, J., J. Burgueno, S. Dreisigacker, M. Vargas, S.A. Herrera-Foessel, M. Lillemo et al. 2007. Association analysis of historical bread wheat germplasm using additive genetic covariance of relatives and population structure. Genetics 177:1889–1913. doi:10.1534/genetics.107.078659

Dunckel, S.M., E.L. Olson, M.N. Rouse, R.L. Bowden, and J.A. Poland. 2015. Genetic mapping of race-specific stem rust resistance in the synthetic hexaploid W7984 × Opata M85 mapping population. Crop Sci. 55:2580–2588. doi:10.2135/cropsci2014.11.0755

Earl, D., and B. vonHoldt. 2012. STRUCTURE HARVESTER: A website and program for visualizing STRUCTURE output and implementing the Evanno method. Conserv. Genet. Resour. 4:359–361. doi:10.1007/s12686-011-9548-7

Ellis, J.G., E.S. Lagudah, W. Spielmeyer, and P.N. Dodds. 2014. The past, present and future of breeding rust resistant wheat. Front. Plant Sci. 5:641. doi:10.3389/fpls.2014.00641

Elshire, R.J., J.C. Glaubitz, Q. Sun, J.A. Poland, K. Kawamoto, E.S. Buckler et al. 2011. A robust, simple genotyping-by-sequencing (GBS) approach for high diversity species. PLoS One 6: e19379. doi:10.1371/journal.pone.0019379

Evanno, G., S. Regnaut, and J. Goudet. 2005. Detecting the number of clusters of individuals using the software structure: A simulation study. Mol. Ecol. 14:2611–2620. doi:10.1111/j.1365-294X.2005.02553.x

Gao, L., M.K. Turner, S. Chao, J. Kolmer, and J.A. Anderson. 2016. Genome wide association study of seedling and adult plant leaf rust resistance in elite spring wheat breeding lines. PLoS One 11:e0148671. doi:10.1371/journal.pone.0148671

Gao, X., L.C. Becker, D.M. Becker, J.D. Starmer, and M.A. Province. 2010. Avoiding the high Bonferroni penalty in genome-wide association studies. Genet. Epidemiol. 34:100–105. doi:10.1002/gepi.20430

Gao, X.Y., J. Stamier, and E.R. Martin. 2008. A multiple testing correction method for genetic association studies using correlated single nucleotide polymorphisms. Genet. Epidemiol. 32:361–369. doi:10.1002/gepi.20310

Ghazvini, H., C.W. Hiebert, J.B. Thomas, and T. Fetch. 2013. Development of a multiple bulked segregant analysis (MBSA) method used to locate a new stem rust resistance gene (*Sr54*) in the winter wheat cultivar Norin 40. Theor. Appl. Genet. 126:443–449. doi:10.1007/s00122-012-1992-6

Guerrero-Chavez, R., K.D. Glover, M.N. Rouse, and J.L. Gonzalez-Hernandez. 2015. Mapping of two loci conferring resistance to wheat stem rust pathogen races TTKSK (Ug99) and TRTTF in the elite hard red spring wheat line SD4279. Mol. Breed. 35:8. doi:10.1007/s11032-015-0198-4

Hirsch, C.N., J.M. Foerster, J.M. Johnson, R.S. Sekhon, G. Muttoni, B. Vaillancourt et al. 2014. Insights into the maize pan-genome and pan-transcriptome. Plant Cell 26:121–135. doi:10.1105/tpc.113.119982

Huang, B.E., A.W. George, K.L. Forrest, A. Kilian, M.J. Hayden, M.K. Morell et al. 2012. A multiparent advanced generation inter-cross population for genetic analysis in wheat. Plant Biotechnol. J. 10:826–839. doi:10.1111/j.1467-7652.2012.00702.x

Jakobsson, M., and N.A. Rosenberg. 2007. CLUMPP: A cluster matching and permutation program for dealing with label switching and multimodality in analysis of population structure. Bioinformatics 23:1801–1806. doi:10.1093/bioinformatics/btm233

Jin, Y., L.J. Szabo, Z.A. Pretorius, R.P. Singh, R. Ward, and T. Fetch. 2008. Detection of virulence to resistance gene *Sr24* within race TTKS of *Puccinia graminis* f. sp *tritici*. Plant Dis. 92:923–926. doi:10.1094/PDIS-92-6-0923

Kislev, M.E. 1982. Stem rust of wheat 3300 years old found in Israel. Science 216:993–994. doi:10.1126/science.216.4549.993

Large, E.C. 1954. Growth stages in cereals illustration of the Feekes scale. Plant Pathol. 3:128–129. doi:10.1111/j.1365-3059.1954.tb00716.x

Maccaferri, M., J. Zhang, P. Bulli, Z. Abate, S. Chao, D. Cantu et al. 2015. A genome-wide association study of resistance to stripe rust (*Puccinia striiformis* f. sp. *tritici*) in a worldwide collection of hexaploid spring wheat (*Triticum aestivum* L.). G3: Genes, Genomes, Genet. 5:449–465. doi:10.1534/g3.114.014563

Mago, R., G. Brown-Guedira, S. Dreisigacker, J. Breen, Y. Jin, R. Singh et al. 2011. An accurate DNA marker assay for stem rust resistance gene *Sr2* in wheat. Theor. Appl. Genet. 122:735–744. doi:10.1007/s00122-010-1482-7

Mago, R., G.J. Lawrence, and J.G. Ellis. 2010. The application of DNA marker and doubled-haploid technology for stacking multiple stem rust resistance genes in wheat. Mol. Breed. 27:329–335. doi:10.1007/s11032-010-9434-0

Mago, R., P. Zhang, S. Vautrin, H. Šimková, U. Bansal, M.-C. Luo et al. 2015. The wheat *Sr50* gene reveals rich diversity at a cereal disease resistance locus. Nature Plants 1:15186. doi:10.1038/nplants.2015.186

MAS Wheat. 2016. Disease resistance. Stem rust resistance. MAS Wheat. http://maswheat.ucdavis.edu/protocols/sr36/ (accessed 15 July 2016)

McIntosh, R., and G. Brown. 1997. Anticipatory breeding for resistance to rust diseases in wheat. Annu. Rev. Phytopathol. 35:311–326. doi:10.1146/annurev.phyto.35.1.311

McIntosh, R.A., J. Dubcovsky, W.J. Rogers, C. Morris, R. Appels and X.C. Xia. 2013. Catalogue of gene symbols for wheat 2013–2014. USDA. https://wheat.pw.usda.gov/GG2/Triticum/wgc/2013/GeneCatalogueIntroduction.pdf (accessed 3 May 2016).

McIntosh, R.A., C.R. Wellings, and R.F. Park. 1995. Wheat rusts: An atlas of resistance. GenesKluwer Academic Publ., Dordrecht, the Netherlands.

Mihalyov, P.D., V.A. Nichols, P. Bulli, M.N. Rouse, and M.O. Pumphrey. 2017. Multi-locus mixed model analysis of stem rust resistance in winter wheat. Plant Genome 10. doi:10.3835/plantgenome2017.01.0001

MLMM software 2012. MLMM. Github. https://github.com/Gregor-Mendel-Institute/mlmm (accessed 26 Feb. 2016).

Naruoka, Y., K. Ando, P. Bulli, K.T. Muleta, S. Rynearson, and M.O. Pumphrey. 2016. Identification and validation of SNP markers linked to the stripe rust resistance gene *Yr5* in wheat. Crop Sci. 56:3055–3065. doi:10.2135/cropsci2016.03.0189

Newcomb, M., P.D. Olivera, M.N. Rouse, L.J. Szabo, J. Johnson, S. Gale et al. 2016. Kenyan isolates of *Puccinia graminis* f. sp. *tritici* from 2008 to 2014: Virulence to *SrTmp* in the Ug99 race group and implications for breeding programs. Phytopathology 106:729–736. doi:10.1094/PHYTO-12-15-0337-R

Olivera, P.D., Y. Jin, M. Rouse, A. Badebo, T. Fetch, R.P. Singh et al. 2012. Races of *Puccinia graminis* f. sp *tritici* with combined virulence to *Sr13* and *Sr9e* in a field stem rust screening nursery in Ethiopia. Plant Dis. 96:623–628. doi:10.1094/PDIS-09-11-0793

Pasam, R., R. Sharma, M. Malosetti, F. van Eeuwijk, G. Haseneyer, B. Kilian et al. 2012. Genome-wide association studies for agronomical traits in a world wide spring barley collection. BMC Plant Biol. 12:16. doi:10.1186/1471-2229-12-16

Pritchard, J.K., M. Stephens, and P. Donnelly. 2000. Inference of population structure using multilocus genotype data. Genetics 155:945–959.

Purcell, S., B. Neale, K. Todd-Brown, L. Thomas, M.A.R. Ferreira, D. Bender et al. 2007. PLINK: A tool set for whole-genome association and population-based linkage analyses. Am. J. Hum. Genet. 81:559–575. doi:10.1086/519795

R Core Team. 2015. R: A language and environment for statistical computing. R Foundation for Statistical Computing, Vienna, Austria.

Roelfs, A. 1985. The cereal rusts. Academic Press, Orlando, FL.

Rouse, M., J. Nirmala, Y. Jin, S. Chao, T. Fetch, Z. Pretorius, et al. 2014. Characterization of *Sr9h*, a wheat stem rust resistance allele effective to Ug99. Theor. Appl. Genet. 127:1681–1688. doi:10.1007/s00122-014-2330-y

Rouse, M.N., I.C. Nava, S. Chao, J.A. Anderson, and Y. Jin. 2012. Identification of markers linked to the race Ug99 effective stem rust resistance gene *Sr28* in wheat (*Triticum aestivum* L.). Theor. Appl. Genet. 125:877–885. doi:10.1007/s00122-012-1879-6

Rouse, M.N., R. Wanyera, P. Njau, and Y. Jin. 2011. Sources of resistance to stem rust race Ug99 in spring wheat germplasm. Plant Dis. 95:762–766. doi:10.1094/PDIS-12-10-0940

Rutkoski, J., J. Benson, Y. Jia, G. Brown-Guedira, J.L. Jannink, and M. Sorrells. 2012. Evaluation of genomic prediction methods for Fusarium head blight resistance in wheat. Plant Genome 5:51–61. doi:10.3835/plantgenome2012.02.0001

Rutkoski, J.E., E.L. Heffner, and M.E. Sorrells. 2011. Genomic selection for durable stem rust resistance in wheat. Euphytica 179:161–173. doi:10.1007/s10681-010-0301-1

Seeholzer, S., T. Tsuchimatsu, T. Jordan, S. Bieri, S. Pajonk, W. Yang et al. 2010. Diversity at the *Mla* powdery mildew resistance locus from cultivated barley reveals sites of positive selection. Mol. Plant Microbe Interact. 23:497–509. doi:10.1094/MPMI-23-4-0497

Segura, V., B.J. Vilhjalmsson, A. Platt, A. Korte, U. Seren, Q. Long et al. 2012. An efficient multi-locus mixed-model approach for genome-wide association studies in structured populations. Nat. Genet. 44:825–830. doi:10.1038/ng.2314

Semagn, K., R. Babu, S. Hearne, and M. Olsen. 2014. Single nucleotide polymorphism genotyping using Kompetitive allele specific PCR (KASP): Overview of the technology and its application in crop improvement. Mol. Breed. 33:1–14. doi:10.1007/s11032-013-9917-x

Simons, K., Z. Abate, S. Chao, W. Zhang, M. Rouse, Y. Jin et al. 2011. Genetic mapping of stem rust resistance gene *Sr13* in tetraploid wheat (*Triticum turgidum* ssp. *durum* L.). Theor. Appl. Genet. 122:649–658. doi:10.1007/s00122-010-1444-0

SimpleM software. 2008. Simple M. SourceForge. http://simplem.sourceforge.net/ (accessed 2 Mar. 2016).

Singh, A., R.E. Knox, R.M. DePauw, A.K. Singh, R.D. Cuthbert, H.L. Campbell et al. 2013. Identification and mapping in spring wheat of genetic factors controlling stem rust resistance and the study of their epistatic interactions across multiple environments. Theor. Appl. Genet. 126:1951–1964. doi:10.1007/s00122-013-2109-6

Singh, R.P., D.P. Hodson, J. Huerta-Espino, Y. Jin, S. Bhavani, P. Njau et al. 2011. The emergence of Ug99 races of the stem rust fungus is a threat to world wheat production. Annu. Rev. Phytopathol. 49:465–481. doi:10.1146/annurev-phyto-072910-095423

Singh, R.P., D.P. Hodson, Y. Jin, E.S. Lagudah, M.A. Ayliffe, S. Bhavani et al. 2015. Emergence and spread of new races of wheat stem rust fungus: Continued threat to food security and prospects of genetic control. Phytopathology 105:872–884. doi:10.1094/PHYTO-01-15-0030-FI

Spindel, J., H. Begum, D. Akdemir, P. Virk, B. Collard, E. Redona et al. 2015. Genomic selection and association mapping in rice (*Oryza sativa*): Effect of trait genetic architecture, training population composition, marker number and statistical model on accuracy of rice genomic selection in elite, tropical rice breeding lines. PLoS Genet. 11:e1005350. doi:10.1371/journal.pgen.1004982

Spindel, J., M. Wright, C. Chen, J. Cobb, J. Gage, S. Harrington et al. 2013. Bridging the genotyping gap: Using genotyping by sequencing (GBS) to add high-density SNP markers and new value to traditional bi-parental mapping and breeding populations. Theor. Appl. Genet. 126:2699–2716. doi:10.1007/s00122-013-2166-x [erratum: 129:201–202].

Spindel, J.E., H. Begum, D. Akdemir, B. Collard, E. Redona, J.L. Jannink et al. 2016. Genome-wide prediction models that incorporate de novo GWAS are a powerful new tool for tropical rice improvement. Heredity 116:395–408. doi:10.1038/hdy.2015.113

Stakman, E.C., D.M. Stewart, and W.Q. Loegering. 1962. Identification of physiologic races of *Puccinia graminis* var. *tricici*. U.S. Gov. Print. Office, Washington, DC.

Thavamanikumar, S., R. Dolferus and B.R. Thumma. 2015. Comparison of genomic selection models to predict flowering time and spike grain number in two hexaploid wheat doubled haploid populations. G3: Genes, Genomes, Genet. 5: 1991–1998. doi:10.1534/g3.115.019745

Tsilo, T.J., Y. Jin, and J.A. Anderson. 2008. Diagnostic microsatellite markers for the detection of stem rust resistance gene *Sr36* in diverse genetic backgrounds of wheat. Crop Sci. 48:253–261. doi:10.2135/cropsci2007.04.0204

Tsilo, T.J., Y. Jin, and J.A. Anderson. 2010. Identification of flanking markers for the stem rust resistance gene *Sr6* in wheat. Crop Sci. 50:1967–1970. doi:10.2135/cropsci2009.11.0648

Turner, M.K., Y. Jin, M.N. Rouse, and J.A. Anderson. 2016a. Stem rust resistance in 'Jagger' winter wheat. Crop Sci. 56:1719–1725. doi:10.2135/cropsci2015.11.0683

Turner, M.K., J.A. Kolmer, M.O. Pumphrey, P. Bulli, S. Chao, and J.A. Anderson. 2016b. Association mapping of leaf rust resistance loci in a spring wheat core collection. Theor. Appl. Genet. 130:345–361. doi:10.1007/s00122-016-2815-y

Wang, S., D. Wong, K. Forrest, A. Allen, S. Chao, B.E. Huang et al. 2014. Characterization of polyploid wheat genomic diversity using a high-density 90 000 single nucleotide polymorphism array. Plant Biotechnol. J. 12:787–796. doi:10.1111/pbi.12183

Weng, Y., P. Azhaguvel, R.N. Devkota, and J.C. Rudd. 2007. PCR-based markers for detection of different sources of 1AL.1RS and 1BL.1RS wheat–rye translocations in wheat background. Plant Breed. 126:482–486. doi:10.1111/j.1439-0523.2007.01331.x

Yu, J., G. Pressoir, W.H. Briggs, I. Vroh Bi, M. Yamasaki, J.F. Doebley et al. 2006. A unified mixed-model method for association mapping that accounts for multiple levels of relatedness. Nat. Genet. 38:203–208. doi:10.1038/ng1702

Yu, L.-X., H. Barbier, M. Rouse, S. Singh, R. Singh, S. Bhavani et al. 2014. A consensus map for Ug99 stem rust resistance loci in wheat. Theor. Appl. Genet. 127:1561–1581. doi:10.1007/s00122-014-2326-7

Yu, L.-X., A. Lorenz, J. Rutkoski, R.P. Singh, S. Bhavani, J. Huerta-Espino et al. 2011. Association mapping and gene-gene interaction for stem rust resistance in CIMMYT spring wheat germplasm. Theor. Appl. Genet. 123:1257–1268. doi:10.1007/s00122-011-1664-y

Yu, L.-X., A. Morgounov, R. Wanyera, M. Keser, S. Singh, and M. Sorrells. 2012. Identification of Ug99 stem rust resistance loci in winter wheat germplasm using genome-wide association analysis. Theor. Appl. Genet. 125:749–758. doi:10.1007/s00122-012-1867-x

Zegeye, H., A. Rasheed, F. Makdis, A. Badebo and F.C. Ogbonnaya. 2014. Genome-wide association mapping for seedling and adult plant resistance to stripe rust in synthetic hexaploid wheat. PLoS One 9: e105593. doi:10.1371/journal.pone.0105593

Zhang, D.D., R.L. Bowden, J.M. Yu, B.F. Carver and G.H. Bai. 2014. Association analysis of stem rust resistance in US winter wheat. PLoS One 9:e103747. doi:10.1371/journal.pone.0103747

Zhu, C., M. Gore, E.S. Buckler, and J. Yu. 2008. Status and prospects of association mapping in plants. Plant Genome 1:5–20. doi:10.3835/plantgenome2008.02.0089

Zurn, J.D., M. Newcomb, M.N. Rouse, Y. Jin, S. Chao, J. Sthapit et al. 2014. High-density mapping of a resistance gene to Ug99 from the Iranian landrace PI 626573. Mol. Breed. 34:1. doi:10.1007/s11032-014-0081-8 [erratum: 35:109].